

STAR: BOOSTING TIME SERIES FOUNDATION MODELS FOR ANOMALY DETECTION THROUGH STATE-AWARE ADAPTER

Hanyin Cheng¹, Ruitong Zhang¹, Yuning Lu¹, Peng Chen², Meng Wang², Yang Shu¹,
 Bin Yang¹, Chenjuan Guo^{1*}

¹East China Normal University

²2012 APPLab, Huawei

{hycheng, rtzhang, ynlu}@stu.ecnu.edu.cn,
 {chenpeng192, wangmeng71}@huawei.com,
 {jlhu, byang, cjguo}@dase.ecnu.edu.cn,

ABSTRACT

While Time Series Foundation Models (TSFMs) have demonstrated remarkable success in Multivariate Time Series Anomaly Detection (MTSAD), however, in real-world industrial scenarios, many time series comprise not only *numerical variables* such as temperature and flow, but also numerous discrete *state variables* that describe the system status, such as valve on/off or day of the week. Existing TSFMs often overlook the distinct categorical nature of state variables and their critical role as conditions, typically treating them uniformly with numerical variables. This inappropriate modeling approach prevents the model from fully leveraging state information and even leads to a significant degradation in detection performance after state variables are integrated. To address this critical limitation, this paper proposes a novel **ST**ate-aware **A**dapte**R** (STAR). STAR is a plug-and-play module designed to enhance the capability of TSFMs in modeling and leveraging state variables during the fine-tuning stage. Specifically, STAR comprises three core components: (1) We design an *Identity-guided State Encoder*, which effectively captures the complex categorical semantics of state variables through a learnable *State Memory*. (2) We propose a *Conditional Bottleneck Adapter*, which dynamically generates low-rank adaptation parameters conditioned on the current state, thereby flexibly injecting the influence of state variables into the backbone model. (3) We also introduce a *Numerical-State Matching* module to more effectively detect anomalies inherent to the state variables themselves. Extensive experiments conducted on real-world datasets demonstrate that STAR can improve the performance of existing TSFMs on MTSAD.

1 INTRODUCTION

In recent years, research into Time Series Foundation Models (TSFMs) has emerged as a significant area of interest. (Shi et al., 2024; Liu et al., 2025; Ekambaram et al., 2024). Researchers are committed to building general-purpose models capable of understanding and processing a diverse range of time series tasks (Liu et al., 2024b; Chen et al., 2025b; Gao et al., 2024). Benefiting from large-scale pre-training, TSFMs can deliver competitive performance without requiring extensive, task-specific fine-tuning. Multivariate Time Series Anomaly Detection (MTSAD), which focuses on identifying abnormal data in multivariate time series, is one of the key downstream tasks targeted by TSFMs (Shentu et al., 2024; Goswami et al., 2024; Wang et al., 2025b). It is applied widely in numerous critical domains, including financial fraud detection, medical disease identification, and cybersecurity threat detection (Wen et al., 2022; Yang et al., 2023a; Kieu et al., 2018).

Although TSFMs have achieved impressive performance in MTSAD, real-world industrial scenarios present more complex data manifestations. In these settings, variables exhibit more intricate forms.

*Corresponding author

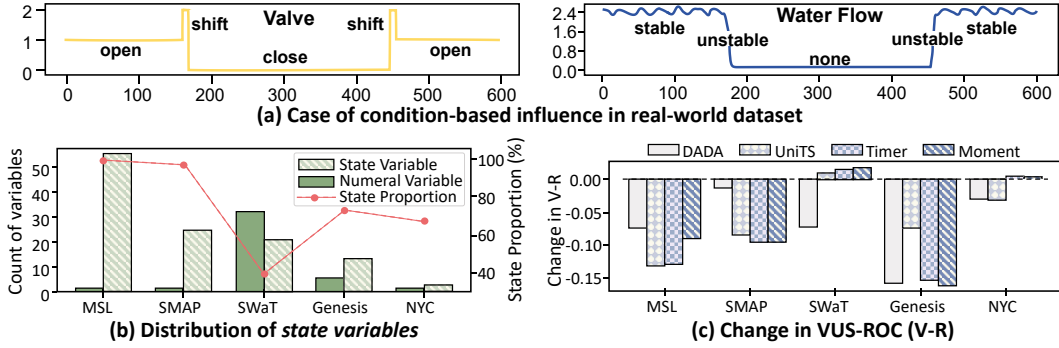


Figure 1: (a) Case of State variables (Valve) and numeral variables (Water Flow) in SWaT. (b) State variables are prevalent in real-world datasets and frequently constitute a substantial proportion. (c) Impact of incorporating state variables on detection performance.

Beyond common *numerical variables* such as temperature, water flow, and velocity, *state variables* also well exist that describe specific system states, such as the open/closed state of a valve (Mathur & Tippenhauer, 2016), the day of the week (Cui et al., 2016), or the positional state of a machine (von Birgelen & Niggemann, 2018). Unlike their numerical counterparts, these state variables are often organized as discrete data, where each value represents a specific category of that state. Moreover, they provide essential context about the system’s operational state and directly influence the numerical variables’ magnitude or temporal patterns. We refer to such influence as *condition-based influence*. For example, as shown in Figure 1a, the valve’s state (open, closed, or shifting) is a precondition for water flow and directly dictates the flow pattern (stable, unstable, or none). Figure 1b illustrates that state variables are widely prevalent in common datasets. However, due to either a lack of pre-training on state variables or uniform modeling for both numerical and state variables, **TSFMs often struggle to handle state variables**. As shown in Figure 1c, when these state variables are incorporated into representative TSFMs through unified modeling, the detection performance fails to improve significantly or suffers a substantial decline.

To address this limitation, we aim to develop a plug-and-play method that enables TSFMs to leverage state variables better, thereby enhancing detection performance and facilitating adaptation to a wider range of industrial scenarios. However, this faces the following challenges:

First, how to extract meaningful embeddings from state variables? State variables possess complex semantics. For instance, within the SWaT (Mathur & Tippenhauer, 2016), several state variables are primarily grouped into three clusters: switches of valves, pumps, and mercury lamps. Within a given group, state variables share similar semantics and exert similar physical influence on the system. Conversely, state variables across different groups are semantically heterogeneous, manifesting in disparate modes of influence. Furthermore, state variables also exhibit distinct temporal patterns, such as the stable periodic patterns of variables representing the day of the week (Cui et al., 2016). In existing foundation models, state variables are typically embedded using linear layers pre-trained on numerical data. While this approach can partially capture the temporal features, it fails to adequately extract the rich and complex semantics inherent in their states.

Second, how to model the condition-based influence of state variables? Different from the correlation among variables (Qiu et al., 2025c; Wu et al., 2025c), the state variables act as preconditions that directly determine the magnitude or temporal patterns of the numerical variables. Therefore, for anomaly detection, it is essential to consider the condition-based influence when processing numerical variables. However, this asymmetric influence between state and numerical variables renders the modeling of condition-based influence a non-trivial task. Some TSFMs, such as UniTS (Gao et al., 2024), model interactions among all variables in a unified manner, this approach erroneously treats them as equivalent, thereby failing to model the condition-based influence effectively.

To close these gaps, we propose **STAR**, a novel STate-aware AdapteR for TSFMs in the MTSAD to better model state variables during the fine-tuning phase. **First**, to better extract embeddings from state variables, we designed a *State Extractor* capable of simultaneously capturing both the state information and temporal patterns of state variables. This module incorporates an *Identity-guided State Encoder* which establishes a small-scale State Memory and retrieves a composite memory’s representation to encode state information guided by both Variable Identity and State Identity. This

method effectively modeling the complex semantics of state variables. **Second**, we propose a *Conditional Bottleneck Adapter* to effectively modeling the condition-based influence. The adapter dynamically generates adaptation parameters and bottleneck size based on state variables to modulate the TSFM’s parameters, thereby directly influencing how the TSFMs process numerical variables. Building upon the aforementioned modules, we can already capture meaningful state information and process numerical variables based on state. Furthermore, we have developed a *Numerical-State Matching* module to more effectively detect anomalies contained within the state variables.

Our contributions are summarized as follows:

- We design a universal State-aware Adapter that equips TSFMs with a more effective mechanism for handling state variables for the MTSAD.
- We propose a novel *Identity-guided State Encoder* in STAR to effectively model the complex homogeneous and heterogeneous semantics of state variables.
- We propose a novel *Conditional Bottleneck Adapter* in STAR, which can flexibly incorporate the condition-based influence of state variables in the TSFMs.
- We conducted extensive experiments on real-world datasets. The results show that STAR effectively improves the performance of TSFMs in MTSAD.

2 RELATED WORKS

2.1 MULTIVARIATE TIME SERIES ANOMALY DETECTION

Classic methods for MTSAD can be classified into non-learning (Breunig et al., 2000; Li et al., 2024b), machine learning (Liu et al., 2008; Ramaswamy et al., 2000), and deep learning (Wu et al., 2025c; Zhong et al., 2025b; Liu et al., 2024a; Liu & Paparrizos, 2024). In particular, methods based on deep learning have seen significant success in recent years. They can be classified into forecasting-based (Deng & Hooi, 2021), reconstruction-based (Wu et al., 2023; Luo & Wang, 2024; Tuli et al., 2022) and contrastive-based methods (Xu et al., 2021; Yang et al., 2023b; Guo et al., 2023). Although some of these models consider variable interactions within a unified modeling framework (Wu et al., 2025c; Xie et al., 2025), or employ specialized modeling for discrete variables (Li et al., 2024a; Chen et al., 2025a), they still treat state variables as mere discrete numerical values, thereby overlooking the condition-based influence of state variables.

2.2 TIME SERIES FOUNDATION MODELS FOR ANOMALY DETECTION

Researchers are actively exploring Foundation Models for various time series analysis tasks, including forecasting (Wang et al., 2025b; Liu et al., 2025; Wang et al., 2024; Das et al., 2024), classification (Chen et al., 2025b), and anomaly detection (Shentu et al., 2024). For anomaly detection, models can be classified into two primary categories: 1) **Task-general model**: These models are typically pre-trained on extensive data, endowing them with excellent representation learning capabilities (Gao et al., 2024; Goswami et al., 2024; Liu et al., 2024b). 2) **Task-specific model**: These models have architectures specifically designed for the anomaly detection task. For instance, to better adapt to anomalous data, DADA (Shentu et al., 2024) employs multiple bottleneck layers of varying sizes for decoding. Additionally, some work has focused on designing adapters to augment TSFMs during fine-tuning phase, such as AdaPTS (Benechehab et al., 2025) and MSFT (Qiao et al., 2025). However, these efforts are primarily concentrated on forecasting tasks, and more importantly, fail to enable TSFMs to better process state variables.

3 STAR

For the task of time series anomaly detection, we consider a time series as $\mathbf{X} = \{\mathbf{X}^n, \mathbf{X}^s\} \in \mathbb{R}^{T \times (C_n + C_s)}$, which consists of C_n numerical variables \mathbf{X}^n and C_s state variables \mathbf{X}^s over T time points. A TSFM is leveraged to identify anomalies in a previously unseen test series \mathbf{X}_{test} either via direct inference or subsequent fine-tuning. Specifically, the model’s goal is to generate a binary prediction sequence $\mathbf{Y}_{\text{test}} = (y_1, y_2, \dots, y_{T_{\text{test}}}) \in \mathbb{R}^{T_{\text{test}}}$. Each element $y_t \in \{0, 1\}$ in this sequence serves as a label, signifying whether the corresponding data point y_t at time t is anomalous.

3.1 OVERVIEW

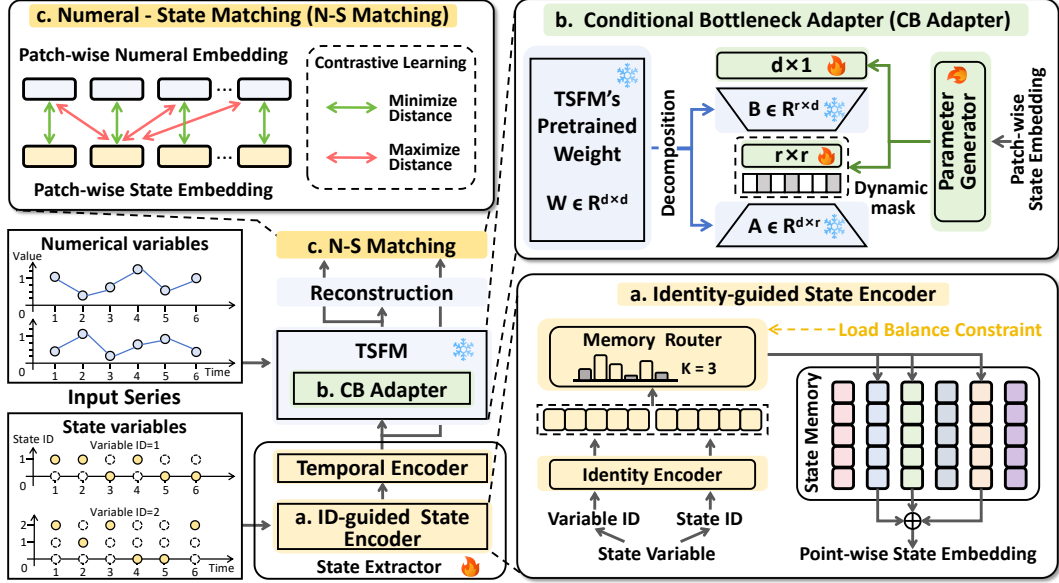


Figure 2: The overview of STAR.

Figure 2 shows the overall architecture of **STAR**, which reconsiders the state variables for TSFMs using the **STate-aware AdapteR**. We shift the processing of state variables from TSFMs to STAR. It mainly consists of three modules: 1) **State Extractor**. Addressing the specific characteristics of state variables, this module simultaneously extracts their state and temporal features and utilizes an *Identity-guided Selective State Encoder* to model the complex semantics of state variables effectively. 2) **Conditional Bottleneck Adapter**. To better model the condition-based influence, we no longer directly model interactions between state and numerical variables. Instead, we use the state variable to modulate the TSFM’s parameters, thereby influencing its processing of numerical variable. 3) **Numeral-State Matching**. To better detect anomalies in the state, we design a contrastive learning based on the degree of matching between numerical and state variables at the patch level. Notably, during the fine-tuning process, the entire Backbone network is frozen, and only STAR is utilized to perform the fine-tuning effectively.

3.2 STATE EXTRACTOR GUIDED BY IDENTITY

The *State Extractor* operates in two sequential stages. First, an *Identity-guided State Encoder* captures state information from the variable identities (indices of state variables) and the state identities (discrete values of state variables) at each time point. Subsequently, a *Temporal Encoder* extracts temporal patterns within each patch.

3.2.1 IDENTITY-GUIDED STATE ENCODER

Formally, state variables are a type of categorical variable, and different state variables can have different cardinality or the number of categories. Most existing methods learn a representation for every individual category via a dedicated, learnable vector to embed the categorical variable (Shan et al., 2016; Hollmann et al., 2025; Li et al., 2025c). This method, however, imposes a substantial parameter burden and learning complexity. More importantly, it fails to account for the similarity or heterogeneity among different state variables.

Inspired by the Mixture of Experts architecture (Zhou et al., 2022; Cai et al., 2025), which uses router networks to select experts for different inputs, we propose a novel approach. Our approach introduces a learnable, compact State Memory, denoted as $S \in \mathbb{R}^{N \times d}$, which consists of N d -dimensional vectors. Under the guidance of variable identities $I_v \in \mathbb{R}^{T \times C_s \times d}$ and state identities $I_s \in \mathbb{R}^{T \times C_s \times d}$, a linear combination of a vector subset from this State Memory is selected to serve as the state representation. We begin by employing a Sinusoidal Encoding (Vaswani et al., 2017) to

transform the variable and state identity into \mathbf{I}_v and \mathbf{I}_s .

$$\mathbf{I}_v[:, i, j] = \begin{cases} \sin\left(\frac{i}{\lambda^{2k/d}}\right), & \text{if } j = 2n \\ \cos\left(\frac{i}{\lambda^{2k/d}}\right), & \text{if } j = 2n + 1 \end{cases}, \quad \mathbf{I}_s[:, i, j] = \begin{cases} \sin\left(\frac{s(i)}{\lambda^{2k/d}}\right), & \text{if } j = 2n \\ \cos\left(\frac{s(i)}{\lambda^{2k/d}}\right), & \text{if } j = 2n + 1 \end{cases} \quad (1)$$

Where λ is a constant, n represents any natural number, and $s(\cdot)$ defines the mapping from a state variable's identity to its state's identity at the corresponding time point. The *Memory Router* leverages \mathbf{I}_v and \mathbf{I}_s to dynamically choose a subset of K vectors from the State Memory. To preserve a continuous gradient flow, we implement the selection mechanism using a soft mask.

$$\mathbf{W}_s = f(\text{concat}(\mathbf{I}_v, \mathbf{I}_s)) \in \mathbb{R}^{T \times C_s \times N}, \quad \boldsymbol{\theta} = \text{topK}(\mathbf{W}_s) \in \mathbb{R}^{T \times C_s \times 1} \quad (2)$$

$$\mathbf{W}_{\text{mask}} = \text{softmax}(\mathbf{W}_s + \log(\text{sigmoid}((\mathbf{W}_s - \boldsymbol{\theta})/\epsilon))) \in \mathbb{R}^{T \times C_s \times N} \quad (3)$$

Where f , implemented as an MLP, learns the selection weights from the concatenated embeddings. The function `topK` returns the K -th largest value, denoted as $\boldsymbol{\theta}$. \mathbf{W}_{mask} represents the weights after applying the soft mask, where all values smaller than $\boldsymbol{\theta}$ are attenuated towards zero. ϵ is a small positive constant that pushes the sigmoid's output to its extremes (0 or 1). The point-wise state embedding $\mathbf{S}_{\text{point}} \in \mathbb{R}^{T \times C_s \times d}$ is obtained via the equation: $\mathbf{S}_{\text{point}} = \mathbf{W}_{\text{mask}} \otimes \mathbf{S}$.

To further promote the comprehensive training of all elements within the State Memory and to prevent routing imbalance, we introduce a constraint based on the Coefficient of Variation (Lovie, 2005). This constraint is applied to both the selection frequency \mathbf{E}_{sel} and the routing importance of each element \mathbf{E}_{imp} to ensure load balancing.

$$\mathbf{E}_{\text{sel}} = \text{avg}(\text{sigmoid}((\mathbf{W}_s - \boldsymbol{\theta})/\epsilon)) \in \mathbb{R}^N, \quad \mathbf{E}_{\text{imp}} = \text{avg}(\mathbf{W}_{\text{mask}}) \in \mathbb{R}^N \quad (4)$$

$$\mathcal{L}_{\text{bal}} = \left(\frac{\text{var}(\mathbf{E}_{\text{sel}})}{\text{avg}(\mathbf{E}_{\text{sel}})}\right)^2 + \left(\frac{\text{var}(\mathbf{E}_{\text{imp}})}{\text{avg}(\mathbf{E}_{\text{sel}})}\right)^2 \quad (5)$$

where $\text{avg}(\cdot)$, $\text{var}(\cdot)$ are functions that compute the mean and variance, respectively. \mathcal{L}_{bal} denotes the load-balancing loss, which is incorporated into the overall training objective.

3.2.2 TEMPORAL ENCODER

Motivated by the observation that state variables often exhibit temporal patterns, such as the strong periodicity of a variable representing the day of the week, we further model the temporal interactions among these embeddings across time to derive patch-wise state embeddings $\mathbf{S}_{\text{patch}}$. Initially, the point-wise state embeddings $\mathbf{S}_{\text{point}}$ are segmented into m patches of length l in a manner consistent with the backbone's configuration, yielding $\mathbf{P} \in \mathbb{R}^{m \times l \times C_s \times d}$. This process comprises two components: intra-patch and inter-patch interaction.

$$\mathbf{P}_{\text{intra}} = f_1(\mathbf{P}) \in \mathbb{R}^{m \times C_s \times d}, \quad \mathbf{P}_{\text{inter}} = f_2(\mathbf{P}_{\text{intra}}) + \mathbf{P}_{\text{intra}} \in \mathbb{R}^{m \times C_s \times d} \quad (6)$$

where $f_1 : \mathbb{R}^{l \times d} \rightarrow \mathbb{R}^d$ aggregates the representations within each patch, and $f_2 : \mathbb{R}^m \rightarrow \mathbb{R}^m$ extracts valuable contextual information for each patch. Each state variable reflects only a partial aspect of the system's information. Therefore, to construct a more holistic representation of the system's overall state, we further perform an aggregation over these variables inside each patch.

$$\mathbf{W}_{\text{agg}} = f_3(\mathbf{P}_{\text{inter}}) \in \mathbb{R}^{m \times C_s}, \quad \mathbf{S}_{\text{patch}} = f_4(\text{sum}(\mathbf{W}_{\text{agg}} \odot \mathbf{P}_{\text{inter}})) \in \mathbb{R}^{m \times d} \quad (7)$$

where $f_3 : \mathbb{R}^d \rightarrow \mathbb{R}^1$ is a function that adaptively computes the aggregation weights, and $f_4 : \mathbb{R}^d \rightarrow \mathbb{R}^d$ serves to refine the resulting fused representation further, \odot denotes element-wise multiplication. For a lightweight implementation, both f_1 , f_2 , f_3 and f_4 are implemented as MLPs.

3.3 CONDITIONAL BOTTLENECK ADAPTER

LoRA (Hu et al., 2022) learn a new matrix product of two low-rank matrices to modulate large-scale models' parameters. Formally, for a pretrained weight matrix $\mathbf{W}_0 \in \mathbb{R}^{d_{\text{in}} \times d_{\text{out}}}$, the weight update $\Delta \mathbf{W}$ is constrained to two low-rank matrix. This process can be formalized as:

$$\mathbf{h} = \mathbf{W}_0 \mathbf{x} + \Delta \mathbf{W} \mathbf{x}, \quad \Delta \mathbf{W} = \mathbf{A} \mathbf{B} \quad (8)$$

where \mathbf{h} and \mathbf{x} denote the input and output of the module, respectively. $\mathbf{A} \in \mathbb{R}^{d_{\text{in}} \times r}$ and $\mathbf{B} \in \mathbb{R}^{d_{\text{out}} \times r}$ are two trainable low-rank matrices, with the rank $r \ll \min(d_{\text{in}}, d_{\text{out}})$.

In a similar vein, we propose the Conditional Bottleneck Adapter. This module perceives the system's state to dynamically generate its parameters and determine its bottleneck size, as illustrated in Figure 2b. The weight update $\Delta \mathbf{W}$ is given by the following equation:

$$\Delta \mathbf{W} = \mathbf{A} \mathbf{R} \mathbf{B} \odot \mathbf{D}, \quad \mathbf{R} \in \mathbb{R}^{r \times r}, \quad \mathbf{D} \in \mathbb{R}^{d_{\text{out}} \times 1} \quad (9)$$

where \mathbf{A} and \mathbf{B} are decomposed from \mathbf{W}_0 , as detailed in Section 3.3.1, and remain frozen. \mathbf{R}, \mathbf{B} are determined by the state variable as detailed in Section 3.3.2.

Notably, inspired by (Shentu et al., 2024), we employ a dynamic mask on the \mathbf{R} matrix to modulate the information bottleneck. This mechanism enables the model to adaptively filter information based on the characteristics of diverse input series.

3.3.1 PRETRAINED WEIGHT DECOMPOSITION

To preserve the performance of the original parameters as much as possible, we employ Singular Value Decomposition (SVD) (Stewart, 1993) to decompose the pretrained weight.

$$\mathbf{U}, \Sigma, \mathbf{V} = \text{SVD}(\mathbf{W}_0), \quad \mathbf{U} \in \mathbb{R}^{d_{\text{in}} \times d_{\text{in}}}, \Sigma \in \mathbb{R}^{d_{\text{in}} \times d_{\text{out}}}, \mathbf{V} \in \mathbb{R}^{d_{\text{out}} \times d_{\text{out}}} \quad (10)$$

where, Σ is the singular value matrix, which we truncate to its leading r values to form the matrix $\Sigma_1 \in \mathbb{R}^{d_{\text{in}} \times r}$ and $\Sigma_2 \in \mathbb{R}^{r \times d_{\text{out}}}$ for the purpose of low-rank approximation. Then we compute the low-rank matrices as :

$$\mathbf{A} = \mathbf{U} \Sigma_1 \in \mathbb{R}^{d_{\text{in}} \times r}, \mathbf{B} = \Sigma_2 \mathbf{V} \in \mathbb{R}^{r \times d_{\text{out}}} \quad (11)$$

3.3.2 PARAMETER GENERATOR AND DYNAMIC MASK

For the t -th patch, we utilize its corresponding $\mathbf{S}_{\text{patch}}^t$ to compute the state-dependent parameters \mathbf{R} and \mathbf{D} . It is worth noting that the \mathbf{R} and \mathbf{D} matrices are patch-specific, as they are dynamically generated based on the distinct state of each individual patch.

$$\mathbf{R}_{\text{init}}, \mathbf{D} = g_1(\mathbf{S}_{\text{patch}}^t), \quad g_1 := \mathbb{R}^d \rightarrow \mathbb{R}^{(r \times r + d_{\text{out}})} \quad (12)$$

To facilitate the adaptive adjustment of the information bottleneck, the \mathbf{R}_{init} matrix is further subjected to a dynamic masking process.

$$\mathbf{R}_{\text{mask}} = g_2(\mathbf{S}_{\text{patch}}^t) \in \mathbb{R}^r, \quad \Gamma = g_3(\mathbf{S}_{\text{patch}}^t) \quad (13)$$

$$\mathbf{M} = \text{sigmoid}((\mathbf{R}_{\text{mask}} - \Gamma)/\epsilon) \in \mathbb{R}^{r \times 1}, \quad \mathbf{R} = \mathbf{M} \odot \mathbf{R}_{\text{init}} \quad (14)$$

where $g_2 := \mathbb{R}^d \rightarrow \mathbb{R}^r$, $g_3 := \mathbb{R}^d \rightarrow \mathbb{R}^1$. g_1, g_2, g_3 are implemented as MLPs. \mathbf{R}_{mask} is score for each row in \mathbf{R} , Γ is a masking threshold. \mathbf{M} serves as the soft mask matrix, where if an element in \mathbf{R}_{mask} is below the threshold Γ , the corresponding elements in \mathbf{M} are driven towards zero.

3.4 PIPELINE WITH NUMERAL - STATE MATCHING

Anomalies may manifest not only as aberrant temporal patterns in numerical variables but also as abnormal conditions within the state variables. Existing TSFMs, however, detect anomalies solely through time series reconstruction. Since state variables are represented as categorical variables, merely reconstructing their state identities is insufficient for accurately identifying state-based anomalies. To address this limitation, we introduce the *Numerical-State Matching* module. This module is designed to detect anomalies by learning the degree of correspondence between numerical variables and their associated state variables.

3.4.1 FINETUNING PHASE.

Constructing positive and negative pairs for contrastive learning by injecting anomalies introduces significant training overhead and makes it difficult to guarantee the effectiveness of the synthetic anomalies (Zhong et al., 2025a; Kim et al., 2025). To circumvent these issues, we adopt a different approach. As shown in Figure 2c, we define a positive pair as the corresponding patch-wise numeral

embedding $\mathbf{N}_{\text{patch}}^t \in \mathbb{R}^d$ and patch-wise state embedding $\mathbf{S}_{\text{patch}}^t \in \mathbb{R}^d$. All other non-corresponding pairings are consequently treated as negative examples. The loss for the Numeral - State Matching Contrastive Learning can be expressed as follows:

$$\mathcal{L}_{\text{match}} = -\frac{1}{M} \sum_{t=1}^M \log\left(\frac{\exp(\text{sim}(\mathbf{N}_{\text{patch}}^t, \mathbf{S}_{\text{patch}}^t)/\tau)}{\sum_{k=1}^M \exp(\text{sim}(\mathbf{N}_{\text{patch}}^k, \mathbf{S}_{\text{patch}}^t)/\tau)}\right) \quad (15)$$

where, M denotes the total number of patches in one batch. $\mathbf{N}_{\text{patch}}^i$ and $\mathbf{S}_{\text{patch}}^i$ are the respective numeral and state embeddings corresponding to the i -th patch. The function $\text{sim}(\cdot)$ is the cosine similarity, and τ is a temperature coefficient used to scale the logits in the contrastive loss.

The overall loss during training is composed of three components: the numerical variable reconstruction loss (\mathcal{L}_{rec}), the load-balancing loss ($\mathcal{L}_{\text{balance}}$), and the Numeral-State Matching loss ($\mathcal{L}_{\text{match}}$). The total loss, $\mathcal{L}_{\text{total}}$, is formulated as: $\mathcal{L}_{\text{total}} = \mathcal{L}_{\text{rec}} + \lambda_1 \mathcal{L}_{\text{balance}} + \lambda_2 \mathcal{L}_{\text{match}}$, where λ_1 and λ_2 are hyperparameters that balance the contribution of each loss term.

3.4.2 INFERENCE PHASE

Anomaly detection is performed in two parts: point-wise *numerical reconstruction* and patch-wise *Numeral-State Matching*. During inference on a test time series, their respective scores, denoted as $\text{score}_{\text{rec}}$ and $\text{score}_{\text{match}}$, are calculated separately.

$$\text{score}_{\text{rec}} = \text{avg}(\text{mse}(\hat{\mathbf{X}}_{\text{test}}^n, \mathbf{X}_{\text{test}}^n)) \in \mathbb{R}^{T_{\text{test}}}, \quad \text{score}_{\text{rec}} = \text{sim}(\mathbf{N}_{\text{patch}}, \mathbf{S}_{\text{patch}}) \in \mathbb{R}^{M_{\text{test}}} \quad (16)$$

where $\text{mse}(\cdot)$ is the Mean Square Error, $\text{sim}(\cdot)$ denotes the cosine similarity, $\hat{\mathbf{X}}^n$ represents the reconstruction output of numerical variables from the backbone, and T_{test} and m_{test} are the total number of time points and patches in the test set, respectively. $\text{avg}(\cdot)$ is an operation that computes the mean value across the variable dimension.

Given that $\text{score}_{\text{rec}}$ and $\text{score}_{\text{match}}$ differ in both temporal granularity and numerical scale, we first apply linear interpolation to $\text{score}_{\text{match}}$ to align their resolutions. Subsequently, the two scores are fused by taking their element-wise product.

$$\text{score}'_{\text{match}} = \text{Linear-Interpolation}(\text{score}_{\text{match}}) \in \mathbb{R}^{T_{\text{test}}} \quad (17)$$

$$\text{score}_{\text{total}} = \text{score}_{\text{rec}} \times \text{softmax}(\text{score}'_{\text{match}}) \in \mathbb{R}^{T_{\text{test}}} \quad (18)$$

Our approach not only detects anomalies in numerical variables but also perceives anomalies in the system state. Furthermore, by leveraging patch-wise similarity computation, the model's capability to detect subsequence anomalies is effectively enhanced.

4 EXPERIMENTS

4.1 EXPERIMENTAL SETTINGS

Datasets We evaluate STAR on various datasets with state variables, including **MSL** (Mars Science Laboratory Dataset) (Hundman et al., 2018), **SMAP** (Soil Moisture Active Passive Dataset) (Hundman et al., 2018), **SWaT** (Secure Water Treatment) (Mathur & Tippenhauer, 2016), **Genesis** (von Birgelen & Niggemann, 2018), and **NYC** (Cui et al., 2016). The statistical details about the datasets are available in Appendix A.1.

Backbone We choose the latest state-of-the-art TSFMs for anomaly detection as backbones, including **DADA** (Shentu et al., 2024), **UniTS** (Gao et al., 2024), **Moment** (Goswami et al., 2024), and **Timer** (Liu et al., 2024b). The detailed description is available in Appendix A.2.

Metrics To circumvent the potential for unfair comparisons arising from the diverse threshold selection methods employed by different TSFMs, we primarily adopt threshold-irrelevant metrics for evaluation. These include the AUC-ROC (A-R), VUS-ROC (V-R), and VUS-PR (V-P) (Paparizos et al., 2022). Meanwhile, the comprehensive evaluation is also supplemented by a range of commonly used metrics mentioned in TAB (Qiu et al., 2025b). The description and implementation details of all metrics are shown in Appendix A.3.

Table 1: Results of adapters for different TFSMs. The better results are highlighted in **bold**.

Dataset	MSL			SMAP			SWaT			Genesis			NYC		
Metric	A-R	V-R	V-P												
DADA	0.702	0.746	0.284	0.406	0.451	0.123	0.814	0.740	0.558	0.802	0.832	0.154	0.492	0.652	0.050
+LoRA	0.721	0.765	0.298	0.420	0.463	0.129	0.807	0.735	0.562	0.784	0.818	0.153	0.514	0.666	0.052
+STAR	0.787	0.803	0.323	0.447	0.490	0.129	0.838	0.753	0.577	0.896	0.911	0.165	0.571	0.701	0.065
UniTS	0.747	0.794	0.296	0.515	0.555	0.145	0.236	0.337	0.126	0.704	0.770	0.017	0.486	0.613	0.044
+LoRA	0.748	0.796	0.298	0.529	0.567	0.148	0.235	0.336	0.125	0.706	0.777	0.018	0.508	0.622	0.049
+STAR	0.776	0.810	0.332	0.535	0.575	0.154	0.242	0.355	0.137	0.809	0.850	0.038	0.595	0.717	0.082
Moment	0.714	0.753	0.281	0.520	0.561	0.145	0.267	0.376	0.185	0.886	0.906	0.155	0.521	0.632	0.045
+LoRA	0.716	0.755	0.287	0.521	0.563	0.145	0.272	0.383	0.190	0.889	0.908	0.184	0.526	0.636	0.045
+STAR	0.771	0.807	0.309	0.524	0.562	0.146	0.283	0.388	0.198	0.949	0.950	0.254	0.576	0.680	0.050
Timer	0.749	0.793	0.299	0.530	0.571	0.149	0.226	0.326	0.125	0.842	0.854	0.100	0.517	0.628	0.043
+LoRA	0.750	0.789	0.311	0.535	0.575	0.155	0.234	0.337	0.126	0.902	0.887	0.158	0.455	0.602	0.039
+STAR	0.786	0.812	0.344	0.538	0.579	0.154	0.244	0.352	0.129	0.931	0.944	0.179	0.541	0.658	0.050

4.2 DETECTION RESULTS

Main results We evaluate our model on five real-world datasets containing state variables, using four TSFMs as backbones. We uniformly use 10% of the downstream data for fine-tuning. The results are summarized in Table 1. For a fair comparison, we evaluated two baseline fine-tuning methods: (1) **Backbone**: standard fine-tuning, and (2) **LoRA**: fine-tuning the base model with LoRA (Hu et al., 2022). It can be seen that LoRA-based fine-tuning offers inconsistent and often marginal performance changes, our method consistently delivers substantial enhancements to the detection performance of TSFMs. Compared to standard fine-tuning, STAR improves the V-R metric on task-specific and task-general TSFMs by 6.93% and 6.07%, respectively. This demonstrates the generalizability of STAR across different types of TSFMs. The validity of our motivation and modeling is further highlighted on the Genesis and NYC, where STAR delivers more improvements of 8.73% and 9.17%, owing to the meaningful physical interpretations of their state variables.

Multi-metrics To ensure a comprehensive comparison, we evaluate the models on more metrics, including Accuracy (ACC), Range-Precision (R-P), Range-Recall (R-R), Range-F1-score (R-F1) (Tatbul et al., 2018), Affiliated-Precision (Aff-P), Affiliated-Recall (Aff-R), Affiliated-F1 (Aff-f1) (Huet et al., 2022), AUC-PR (A-P), R-AUC-PR (R-A-P), R-AUC-ROC (R-A-R) (Paparrizos et al., 2022). Table 2 shows that STAR yields performance improvements across the majority of metrics.

Table 2: Multi-metrics results on real-world datasets. The better results are highlighted in **bold**.

Dataset	Method	Threshold-relevant							Threshold-irrelevant						
		ACC	R-P	R-R	R-F1	Aff-P	Aff-R	Aff-F1	A-R	A-P	R-A-R	R-A-P	V-R	V-P	
MSL	DADA	0.814	0.179	0.288	0.221	0.603	0.981	0.747	0.702	0.232	0.752	0.290	0.746	0.284	
	+STAR	0.822	0.164	0.346	0.223	0.694	0.952	0.803	0.790	0.276	0.811	0.337	0.807	0.331	
	UniTS	0.747	0.197	0.261	0.224	0.649	0.996	0.786	0.747	0.222	0.802	0.303	0.794	0.296	
	+STAR	0.816	0.185	0.337	0.239	0.692	0.955	0.803	0.776	0.255	0.815	0.341	0.810	0.332	
Genesis	DADA	0.987	0.333	0.162	0.218	0.835	0.953	0.890	0.802	0.175	0.844	0.152	0.832	0.154	
	+STAR	0.996	0.571	0.172	0.264	0.895	0.969	0.930	0.896	0.159	0.921	0.156	0.911	0.165	
	UniTS	0.977	0.031	0.165	0.058	0.704	0.976	0.818	0.704	0.017	0.791	0.018	0.770	0.017	
	+STAR	0.995	0.154	0.156	0.155	0.807	0.949	0.872	0.809	0.047	0.861	0.039	0.850	0.038	

4.3 MODEL ANALYSIS

Ablation Study To analyze the contribution of each module, we conducted an ablation study, detailed in Table 3. Row 1 shows the standard fine-tuning, while Rows 2-6 illustrate the performance

Table 3: Ablation studies for STAR. The better results are highlighted in **bold**.

ID-guided State Encoder	CB Adapter	N - S Matching	MSL				Genesis				
			DADA		UniTS		DADA		UniTS		
			V-R	V-P	V-R	V-P	V-R	V-P	V-R	V-P	
1	✗	✗	✗	0.746	0.284	0.794	0.296	0.832	0.154	0.770	0.017
2	✗	✓	✗	0.762	0.295	0.792	0.299	0.855	0.154	0.784	0.022
3	✗	✗	✓	0.755	0.290	0.800	0.298	0.841	0.157	0.780	0.019
4	✓	✓	✗	0.803	0.323	0.807	0.311	0.872	0.156	0.819	0.021
5	✓	✗	✓	0.760	0.295	0.805	0.321	0.854	0.150	0.805	0.024
6	✓	✓	✓	0.807	0.331	0.810	0.332	0.911	0.165	0.850	0.038

✗ indicates a module removed, and ✓ indicates a module added.

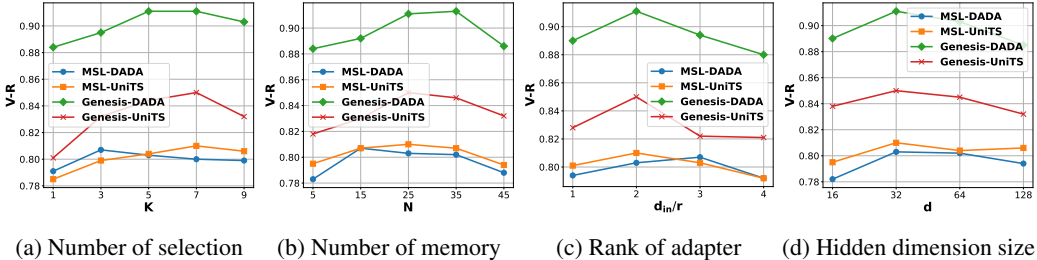


Figure 3: Parameter sensitivity studies of main hyper-parameters in STAR.

when integrating specific modules of STAR with the backbone. We have the following observations: (1) A comparison of rows 1-3 reveals that both the *Conditional Bottleneck Adapter* (*CB Adapter*) and the *Numerical-State Matching* (*N-S Matching*) module can enhance the backbone’s performance to a certain degree. This limited improvement can likely be attributed to the lack of meaningful state information. (2) In Rows 4 and 5, the addition of the *ID-guided State Encoder* results in a more pronounced performance enhancement with the two modules. This validates the effectiveness of the *ID-guided State Encoder* in capturing complex state information. (3) The combination of all three modules creates a virtuous cycle, resulting in the best performance, as shown in Row 6. Specifically, the *N-S Matching* module optimizes the state representations, which in turn enhances the effectiveness of the other modules.

Parameter Sensitivity We study the parameter sensitivity of STAR, including the number of selected vectors in *Memory Router* (K), the total number of memory vectors (N), the rank of the adapter (r), and the hidden dimension size of the adapter (d). To enhance the flexibility of STAR, we search for the value of d_{in}/r directly, rather than searching for r itself. Figure 3a shows the impact of K . In most cases, a smaller K is insufficient for effective learning. We typically select 7 as the preferred option. Besides, Figure 3b illustrates the impact of N . Common choices for this value are 15 or 25. This approach is more lightweight compared to defining a learnable vector for each state of each state variable (Shan et al., 2016). As shown in Figure 3c, by reducing the d_{in} to $d_{in}/2$ or $d_{in}/3$, we can achieve a balance between efficiency and effectiveness. Figure 3d indicates that a large hidden dimension is not required, thus avoiding substantial additional computational costs.

More Analysis To demonstrate the applicability of STAR, we also evaluated its performance on datasets containing solely numerical variables (B.1). We further visualize the *Identity-guided State Encoder* to validate its effectiveness (B.2). Moreover, we present a case study to demonstrate the importance of state variables for anomaly detection (B.3).

5 CONCLUSION

In this study, we propose a novel STate-aware AdapteR (STAR) for TSFM in MTSAD. STAR is a plug-and-play module designed to address the failure of TSFMs to handle state variables during the fine-tuning stage. We propose Identity-guided State Encoder and Conditional Bottleneck Adapter to capture the complex semantics of states and the conditional influence of state variables, respectively.

REFERENCES

Ahmed Abdulaal, Zhuanghua Liu, and Tomer Lancewicki. Practical approach to asynchronous multivariate time series anomaly detection and localization. In *Proceedings of the 27th ACM SIGKDD conference on knowledge discovery & data mining*, pp. 2485–2494, 2021.

Abdelhakim Benechehab, Vasilii Feofanov, Giuseppe Paolo, Albert Thomas, Maurizio Filippone, and Balázs Kégl. Adapts: Adapting univariate foundation models to probabilistic multivariate time series forecasting. *arXiv preprint arXiv:2502.10235*, 2025.

Markus M Breunig, Hans-Peter Kriegel, Raymond T Ng, and Jörg Sander. LOF: identifying density-based local outliers. In *Proceedings of the 2000 ACM SIGMOD international conference on Management of data*, pp. 93–104, 2000.

Weilin Cai, Juyong Jiang, Fan Wang, Jing Tang, Sunghun Kim, and Jiayi Huang. A survey on mixture of experts in large language models. *IEEE Transactions on Knowledge and Data Engineering*, 2025.

Junhao Chen, Chunhui Zhao, Pengyu Song, and Min Xie. Unified low-dimensional subspace analysis of continuous and binary variables for industrial process monitoring. *IEEE Transactions on Cybernetics*, 2025a.

Yuxuan Chen, Shanshan Huang, Yunyao Cheng, Peng Chen, Zhongwen Rao, Yang Shu, Bin Yang, Lujia Pan, and Chenjuan Guo. AimTS: Augmented series and image contrastive learning for time series classification. In *ICDE*, 2025b.

Yuwei Cui, Chetan Surpur, Subutai Ahmad, and Jeff Hawkins. A comparative study of htm and other neural network models for online sequence learning with streaming data. In *IJCNN*, pp. 1530–1538, 2016.

Abhimanyu Das, Weihao Kong, Rajat Sen, and Yichen Zhou. A decoder-only foundation model for time-series forecasting. In *Forty-first International Conference on Machine Learning*, 2024.

Jesse Davis and Mark Goadrich. The relationship between precision-recall and roc curves. In *Proceedings of the international conference on machine learning*, pp. 233–240, 2006.

Ailin Deng and Bryan Hooi. Graph neural network-based anomaly detection in multivariate time series. In *Proceedings of the AAAI conference on artificial intelligence*, volume 35, pp. 4027–4035, 2021.

Vijay Ekambaram, Arindam Jati, Pankaj Dayama, Sumanta Mukherjee, Nam Nguyen, Wesley M Gifford, Chandra Reddy, and Jayant Kalagnanam. Tiny time mixers (ttms): Fast pre-trained models for enhanced zero/few-shot forecasting of multivariate time series. *Advances in Neural Information Processing Systems*, 37:74147–74181, 2024.

Tom Fawcett. An introduction to roc analysis. *Pattern recognition letters*, 27(8):861–874, 2006.

Cheng Feng and Pengwei Tian. Time series anomaly detection for cyber-physical systems via neural system identification and bayesian filtering. In *Proceedings of the 27th ACM SIGKDD conference on knowledge discovery & data mining*, pp. 2858–2867, 2021.

Shanghua Gao, Teddy Koker, Owen Queen, Thomas Hartvigsen, Theodoros Tsiligkaridis, and Marinka Zitnik. Units: Building a unified time series model. *arXiv*, 2024. URL <https://arxiv.org/pdf/2403.00131.pdf>.

Mononito Goswami, Konrad Szafer, Arjun Choudhry, Yifu Cai, Shuo Li, and Artur Dubrawski. Moment: A family of open time-series foundation models. *arXiv preprint arXiv:2402.03885*, 2024.

Xiaojun Guo, Yifei Wang, Tianqi Du, and Yisen Wang. Contranorm: A contrastive learning perspective on oversmoothing and beyond. In *The Eleventh International Conference on Learning Representations*, 2023.

Noah Hollmann, Samuel Müller, Lennart Purucker, Arjun Krishnakumar, Max Körfer, Shi Bin Hoo, Robin Tibor Schirrmeister, and Frank Hutter. Accurate predictions on small data with a tabular foundation model. *Nature*, 637(8045):319–326, 2025.

Edward J Hu, Phillip Wallis, Zeyuan Allen-Zhu, Yuanzhi Li, Shean Wang, Lu Wang, Weizhu Chen, et al. Lora: Low-rank adaptation of large language models. In *International Conference on Learning Representations*, 2022.

Alexis Huet, Jose Manuel Navarro, and Dario Rossi. Local evaluation of time series anomaly detection algorithms. In *Proceedings of the ACM SIGKDD international conference on knowledge discovery & data mining*, pp. 635–645, 2022.

Kyle Hundman, Valentino Constantinou, Christopher Laporte, Ian Colwell, and Tom Soderstrom. Detecting spacecraft anomalies using lstms and nonparametric dynamic thresholding. In *SIGKDD*, pp. 387–395, 2018.

Tung Kieu, Bin Yang, and Christian S Jensen. Outlier detection for multidimensional time series using deep neural networks. In *2018 19th IEEE International Conference on Mobile Data Management (MDM)*, 2018.

HyunGi Kim, Jisoo Mok, Dongjun Lee, Jaihyun Lew, Sungjae Kim, and Sungroh Yoon. Causality-aware contrastive learning for robust multivariate time-series anomaly detection. In *Forty-second International Conference on Machine Learning*, 2025.

Junxian Li, Keke Huang, Dehao Wu, Yishun Liu, Chunhua Yang, and Weihua Gui. Hybrid variable dictionary learning for monitoring continuous and discrete variables in manufacturing processes. *Control Engineering Practice*, 149:105970, 2024a.

Leyang Li, Shilin Lu, Yan Ren, and Adams Wai-Kin Kong. Set you straight: Auto-steering denoising trajectories to sidestep unwanted concepts. *arXiv preprint arXiv:2504.12782*, 2025a.

Xiang Li, Yangfan He, Shuaishuai Zu, Zhengyang Li, Tianyu Shi, Yiting Xie, and Kevin Zhang. Multi-modal large language model with rag strategies in soccer commentary generation. In *WACV*, pp. 6197–6206, 2025b.

Xiaopeng Li, Shasha Li, Shezheng Song, Huijun Liu, Bin Ji, Xi Wang, Jun Ma, Jie Yu, Xiaodong Liu, Jing Wang, et al. Swea: Updating factual knowledge in large language models via subject word embedding altering. In *Proceedings of the AAAI Conference on Artificial Intelligence*, volume 39, pp. 24494–24502, 2025c.

Yijie Li, Hewei Wang, and Aggelos Katsaggelos. CPDR: Towards Highly-Efficient Salient Object Detection via Crossed Post-decoder Refinement. In *35th British Machine Vision Conference 2024, BMVC 2024, Glasgow, UK, November 25-28, 2024*, 2024b.

Zhe Li, Xiangfei Qiu, Peng Chen, Yihang Wang, Hanyin Cheng, Yang Shu, Jilin Hu, Chenjuan Guo, Aoying Zhou, Christian S. Jensen, and Bin Yang. Tsfm-bench: A comprehensive and unified benchmark of foundation models for time series forecasting. In *SIGKDD*, pp. 5595–5606, 2025d.

Fei Tony Liu, Kai Ming Ting, and Zhi-Hua Zhou. Isolation forest. In *Proceedings of the 2008 IEEE international conference on data mining*, pp. 413–422, 2008.

Qinghua Liu and John Paparrizos. The elephant in the room: Towards a reliable time-series anomaly detection benchmark. In *NeurIPS*, 2024.

Qinghua Liu, Paul Boniol, Themis Palpanas, and John Paparrizos. Time-series anomaly detection: Overview and new trends. *Proc. VLDB Endow.*, 17(12):4229–4232, 2024a.

Yong Liu, Haoran Zhang, Chenyu Li, Xiangdong Huang, Jianmin Wang, and Mingsheng Long. Timer: Generative pre-trained transformers are large time series models. In *International Conference on Machine Learning*, pp. 32369–32399. PMLR, 2024b.

Yong Liu, Guo Qin, Zhiyuan Shi, Zhi Chen, Caiyin Yang, Xiangdong Huang, Jianmin Wang, and Mingsheng Long. Sundial: A family of highly capable time series foundation models. *arXiv preprint arXiv:2502.00816*, 2025.

Pat Lovie. Coefficient of variation. *Encyclopedia of statistics in behavioral science*, 2005.

Shilin Lu, Yanzhu Liu, and Adams Wai-Kin Kong. Tf-icon: Diffusion-based training-free cross-domain image composition. In *ICCV*, pp. 2294–2305, 2023.

Shilin Lu, Zilan Wang, Leyang Li, Yanzhu Liu, and Adams Wai-Kin Kong. Mace: Mass concept erasure in diffusion models. In *CVPR*, pp. 6430–6440, 2024a.

Shilin Lu, Zihan Zhou, Jiayou Lu, Yuanzhi Zhu, and Adams Wai-Kin Kong. Robust watermarking using generative priors against image editing: From benchmarking to advances. *arXiv preprint arXiv:2410.18775*, 2024b.

Donghao Luo and Xue Wang. Moderntcn: A modern pure convolution structure for general time series analysis. In *The Twelfth International Conference on Learning Representations*, 2024.

Aditya P Mathur and Nils Ole Tippenhauer. Swat: A water treatment testbed for research and training on ics security. In *CySWater*, pp. 31–36, 2016.

John Paparrizos, Paul Boniol, Themis Palpanas, Ruey S Tsay, Aaron Elmore, and Michael J Franklin. Volume under the surface: a new accuracy evaluation measure for time-series anomaly detection. *Proceedings of the VLDB Endowment*, 15(11):2774–2787, 2022.

Zhongzheng Qiao, Chenghao Liu, Yiming Zhang, Ming Jin, Quang Pham, Qingsong Wen, PN Suganthan, Xudong Jiang, and Savitha Ramasamy. Multi-scale finetuning for encoder-based time series foundation models. *arXiv preprint arXiv:2506.14087*, 2025.

Xiangfei Qiu, Jilin Hu, Lekui Zhou, Xingjian Wu, Junyang Du, Buang Zhang, Chenjuan Guo, Aoying Zhou, Christian S. Jensen, Zhenli Sheng, and Bin Yang. TFB: Towards comprehensive and fair benchmarking of time series forecasting methods. In *Proc. VLDB Endow.*, pp. 2363–2377, 2024.

Xiangfei Qiu, Xiuwen Li, Ruiyang Pang, Zhicheng Pan, Xingjian Wu, Liu Yang, Jilin Hu, Yang Shu, Xuesong Lu, Chengcheng Yang, Chenjuan Guo, Aoying Zhou, Christian S. Jensen, and Bin Yang. EasyTime: Time series forecasting made easy. In *ICDE*, 2025a.

Xiangfei Qiu, Zhe Li, Wanghui Qiu, Shiyan Hu, Lekui Zhou, Xingjian Wu, Zhengyu Li, Chenjuan Guo, Aoying Zhou, Zhenli Sheng, Jilin Hu, Christian S. Jensen, and Bin Yang. Tab: Unified benchmarking of time series anomaly detection methods. In *Proc. VLDB Endow.*, pp. 2775–2789, 2025b.

Xiangfei Qiu, Xingjian Wu, Yan Lin, Chenjuan Guo, Jilin Hu, and Bin Yang. DUET: Dual clustering enhanced multivariate time series forecasting. In *SIGKDD*, pp. 1185–1196, 2025c.

Sridhar Ramaswamy, Rajeev Rastogi, and Kyuseok Shim. Efficient algorithms for mining outliers from large data sets. In *Proceedings of the 2000 ACM SIGMOD international conference on management of data*, pp. 427–438, 2000.

Ying Shan, T Ryan Hoens, Jian Jiao, Haijing Wang, Dong Yu, and JC Mao. Deep crossing: Web-scale modeling without manually crafted combinatorial features. In *Proceedings of the 22nd ACM SIGKDD international conference on knowledge discovery and data mining*, pp. 255–262, 2016.

Qichao Shentu, Beibu Li, Kai Zhao, Yang Shu, Zhongwen Rao, Lujia Pan, Bin Yang, and Chenjuan Guo. Towards a general time series anomaly detector with adaptive bottlenecks and dual adversarial decoders. *arXiv preprint arXiv:2405.15273*, 2024.

Xiaoming Shi, Shiyu Wang, Yuqi Nie, Dianqi Li, Zhou Ye, Qingsong Wen, and Ming Jin. Timemoe: Billion-scale time series foundation models with mixture of experts. *arXiv e-prints*, pp. arXiv–2409, 2024.

Gilbert W Stewart. On the early history of the singular value decomposition. *SIAM review*, 35(4): 551–566, 1993.

Nesime Tatbul, Tae Jun Lee, Stan Zdonik, Mejbah Alam, and Justin Gottschlich. Precision and recall for time series. *Advances in neural information processing systems*, 31, 2018.

Shreshth Tuli, Giuliano Casale, and Nicholas R Jennings. Tranad: Deep transformer networks for anomaly detection in multivariate time series data. *arXiv preprint arXiv:2201.07284*, 2022.

Ashish Vaswani, Noam Shazeer, Niki Parmar, Jakob Uszkoreit, Llion Jones, Aidan N. Gomez, Łukasz Kaiser, and Illia Polosukhin. Attention is all you need. In *Neural Information Processing Systems NeurIPS*, pp. 5998–6008, 2017.

Alexander von Birgelen and Oliver Niggemann. Anomaly detection and localization for cyber-physical production systems with self-organizing maps. *IMPROVE-Innovative Modelling Approaches for Production Systems to Raise Validatable Efficiency: Intelligent Methods for the Factory of the Future*, pp. 55–71, 2018.

Ruoyu Wang, Yangfan He, Tengjiao Sun, Xiang Li, and Tianyu Shi. Unitmge: Uniform text-motion generation and editing model via diffusion. In *WACV*, pp. 6104–6114, 2025a.

Yihang Wang, Yuying Qiu, Peng Chen, Kai Zhao, Yang Shu, Zhongwen Rao, Lujia Pan, Bin Yang, and Chenjuan Guo. ROSE: Register assisted general time series forecasting with decomposed frequency learning. *arXiv preprint arXiv:2405.17478*, 2024.

Yihang Wang, Yuying Qiu, Peng Chen, Yang Shu, Zhongwen Rao, Lujia Pan, Bin Yang, and Chenjuan Guo. Lightgts: A lightweight general time series forecasting model. *arXiv preprint arXiv:2506.06005*, 2025b.

Qingsong Wen, Linxiao Yang, Tian Zhou, and Liang Sun. Robust time series analysis and applications: An industrial perspective. In *Proceedings of the 28th ACM SIGKDD Conference on Knowledge Discovery and Data Mining*, pp. 4836–4837, 2022.

Haixu Wu, Tengge Hu, Yong Liu, Hang Zhou, Jianmin Wang, and Mingsheng Long. Timesnet: Temporal 2d-variation modeling for general time series analysis. In *ICLR*, 2023.

Xingjian Wu, Xiangfei Qiu, Hongfan Gao, Jilin Hu, Bin Yang, and Chenjuan Guo. K²VAE: A koopman-kalman enhanced variational autoencoder for probabilistic time series forecasting. In *ICML*, 2025a.

Xingjian Wu, Xiangfei Qiu, Zhengyu Li, Yihang Wang, Jilin Hu, Chenjuan Guo, Hui Xiong, and Bin Yang. CATCH: Channel-aware multivariate time series anomaly detection via frequency patching. In *ICLR*, 2025b.

Xingjian Wu, Xiangfei Qiu, Zhengyu Li, Yihang Wang, Jilin Hu, Chenjuan Guo, Hui Xiong, and Bin Yang. Catch: Channel-aware multivariate time series anomaly detection via frequency patching. In *International Conference on Learning Representations (ICLR)*, 2025c.

Xinle Wu, Xingjian Wu, Bin Yang, Lekui Zhou, Chenjuan Guo, Xiangfei Qiu, Jilin Hu, Zhenli Sheng, and Christian S. Jensen. AutoCTS++: zero-shot joint neural architecture and hyperparameter search for correlated time series forecasting. *VLDB J.*, 33(5):1743–1770, 2024.

Yongzheng Xie, Hongyu Zhang, and Muhammad Ali Babar. Multivariate time series anomaly detection by capturing coarse-grained intra-and inter-variate dependencies. In *Proceedings of the ACM on Web Conference 2025*, pp. 697–705, 2025.

Jiehui Xu, Haixu Wu, Jianmin Wang, and Mingsheng Long. Anomaly Transformer: Time series anomaly detection with association discrepancy. In *International Conference on Learning Representations*, 2021.

Ronghui Xu, Hanyin Cheng, Chenjuan Guo, Hongfan Gao, Jilin Hu, Sean Bin Yang, and Bin Yang. Mm-path: Multi-modal, multi-granularity path representation learning. In *SIGKDD*, pp. 1703–1714, 2025.

Chen Yang, Yangfan He, Aaron Xuxiang Tian, Dong Chen, Jianhui Wang, Tianyu Shi, Arsalan Heydarian, and Pei Liu. Wcdt: World-centric diffusion transformer for traffic scene generation. *arXiv preprint arXiv:2404.02082*, 2024.

Yiyuan Yang, Rongshang Li, Qiquan Shi, Xijun Li, Gang Hu, Xing Li, and Mingxuan Yuan. Sgdp: A stream-graph neural network based data prefetcher. In *2023 International Joint Conference on Neural Networks (IJCNN)*, pp. 1–8, 2023a.

Yiyuan Yang, Chaoli Zhang, Tian Zhou, Qingsong Wen, and Liang Sun. Dcdetector: Dual attention contrastive representation learning for time series anomaly detection. In *Proceedings of the 29th ACM SIGKDD Conference on Knowledge Discovery and Data Mining*, pp. 3033–3045, 2023b.

Susik Yoon, Jae-Gil Lee, and Byung Suk Lee. Ultrafast local outlier detection from a data stream with stationary region skipping. In *SIGKDD*, pp. 1181–1191, 2020.

Zhijie Zhong, Zhiwen Yu, Xing Xi, Yue Xu, Wenming Cao, Yiyuan Yang, Kaixiang Yang, and Jane You. Simad: A simple dissimilarity-based approach for time-series anomaly detection. *IEEE Transactions on Neural Networks and Learning Systems*, 2025a.

Zhijie Zhong, Zhiwen Yu, Xing Xi, Yue Xu, Wenming Cao, Yiyuan Yang, Kaixiang Yang, and Jane You. Simad: A simple dissimilarity-based approach for time-series anomaly detection. *IEEE Transactions on Neural Networks and Learning Systems*, 2025b.

Yanqi Zhou, Tao Lei, Hanxiao Liu, Nan Du, Yanping Huang, Vincent Zhao, Andrew M Dai, Quoc V Le, James Laudon, et al. Mixture-of-experts with expert choice routing. *Advances in Neural Information Processing Systems*, 35:7103–7114, 2022.

Yiyang Zhou, Yangfan He, Yaofeng Su, Siwei Han, Joel Jang, Gedas Bertasius, Mohit Bansal, and Huaxiu Yao. Reagent-v: A reward-driven multi-agent framework for video understanding. *arXiv preprint arXiv:2506.01300*, 2025.

A EXPERIMENTAL DETAILS

A.1 DATASETS

To evaluate our method, we selected five classic real-world multivariate anomaly detection datasets: 1) **MSL** (Hundman et al., 2018): Spacecraft incident and anomaly data from the MSL Curiosity rover. 2) **SMAP** (Hundman et al., 2018): Presents the soil samples and telemetry information used by the Mars rover. 3) **SWAT** (Mathur & Tippenhauer, 2016): Obtained from 51 sensors of the critical infrastructure system under continuous operations. 4) **Genesis** (von Birgelen & Niggemann, 2018): A sensor and control signals dataset collected from cyber-physical production systems. 5) **NYC** (Cui et al., 2016): The Transportation dataset provides information on taxi and ride-hailing trips in New York. Each of these datasets contains a significant number of *state variables*, with detailed statistics presented in Table 4.

Table 4: Statistics of multivariate datasets (AR: anomaly ratio).

Dataset	Domain	Numerical Numbers	State Numbers	AR (%)	Avg Total Length	Avg Test Length
MSL	Spacecraft	1	54	5.88	132,046	73,729
SMAP	Spacecraft	1	24	9.72	562,800	427,617
SWAT	Water treatment	28	23	5.78	944,919	449,919
Genesis	Machinery	5	13	0.31	16,220	12,616
NYC	Transport	1	2	0.57	17,520	4,416

A.2 TIME SERIES FOUNDATION MODELS FOR ANOMALY DETECTION

In recent years, deep learning (Wu et al., 2025a; Qiu et al., 2025c; Wu et al., 2024) has achieved widespread success in tasks such as image (Lu et al., 2024a; 2023; 2024b; Zhou et al., 2025), language (Li et al., 2025b; Wang et al., 2025a), and spatio-temporal analysis (Xu et al., 2025; Li et al., 2025a; Yang et al., 2024; Wang et al., 2025a; Qiu et al., 2025a; Wu et al., 2025b).

In the realm of time series analysis, numerous models have surfaced in recent years (Qiu et al., 2025a; Wu et al., 2025b; Qiu et al., 2024; Li et al., 2025d). We choose models which designed for multi-task or specialised for anomaly detection, including task-specific model DADA (Shentu et al., 2024) and task-general models: UniTS (Gao et al., 2024), Moment (Goswami et al., 2024), Timer (Liu et al., 2024b). The specific descriptions for each of these models are listed in Table 5.

Table 5: Descriptions of Time Series Foundation Models for Anomaly Detection in experiments.

Models	Descriptions
DADA	DADA is a general time series anomaly detector pre-trained on multi-domain data, utilizing adaptive bottlenecks and dual adversarial decoders. It is designed to detect by learning to differentiate between normal and abnormal patterns.
UniTS	UniTS is a unified, multi-task transformer model that uses task tokenization to handle a variety of time series tasks like forecasting, classification, imputation, and anomaly detection within a single framework.
Moment	Moment is a transformer system pre-trained on a masked time series task. It reconstructs masked portions of time series for tasks like forecasting, classification, anomaly detection, and imputation.
Timer	Timer is a GPT-style autoregressive model for time series analysis, predicting the next token in single-series sequences. It supports tasks like forecasting, imputation, and anomaly detection across different time series.

A.3 METRICS FOR TIME SERIES ANOMALY DETECTION

The metrics used for evaluation can be divided into two categories: Threshold-relevant and Threshold-irrelevant. Threshold-relevant metrics depend on threshold parameters to convert

anomaly scores into anomaly labels. Among them, Threshold-irrelevant metrics, on the other hand, evaluate the performance of the model based on the raw anomaly scores it generates. Please refer to Table 6 for an overview of these metrics.

Table 6: Overview of evaluation metrics.

Category	Metric	Abbreviation	Short summary
Threshold-relevant	Accuracy	Acc	Measures the proportion of correct predictions among the total number of predictions.
	Range-Precision	R-P Tabul et al. (2018)	These metrics' definitions consider several factors: the ratio of detected anomaly subsequences to the total number of anomalies,
	Range-Recall	R-R Tabul et al. (2018)	the ratio of detected point outliers to total point outliers, the relative position of true positives within each anomaly subsequence,
	Range-F1-score	R-F1 Tabul et al. (2018)	and the number of fragmented prediction regions corresponding to one real anomaly subsequence.
Threshold-irrelevant	Affiliated-Precision	Aff-P Huet et al. (2022)	These metrics' definitions are the extension of the classical precision/recall/f1-score for time series anomaly detection that is
	Affiliated-Recall	Aff-R Huet et al. (2022)	local (each ground truth event is considered separately), parameter-free, and applicable generically on both point and subsequence anomalies. Besides the construction of these metrics makes them both theoretically principled and practically useful.
	Affiliated-F1-score	Aff-F1 Huet et al. (2022)	
Threshold-irrelevant	AUC-PR	A-P Davis & Goadrich (2006)	Measures the area under the curve corresponding to Recall on the x-axis and Precision on the y-axis at various threshold settings.
	AUC-ROC	A-R Fawcett (2006)	Measures the area under the curve corresponding to FPR on the x-axis and TPR on the y-axis at various threshold settings.
	R-AUC-PR	R-A-P Paparrizos et al. (2022)	They mitigate the issue that AUC-PR and AUC-ROC are designed for point-based anomaly detection, where each point is
	R-AUC-ROC	R-A-R Paparrizos et al. (2022)	assigned equal weight in calculating the overall AUC. This makes them unsuitable for evaluating subsequence anomalies.
	VUS-PR	V-PR Paparrizos et al. (2022)	VUS is an extension of the ROC and PR curves. It introduces a buffer region at the outliers' boundaries, thereby accommodating
	VUS-ROC	V-ROC Paparrizos et al. (2022)	the false tolerance of labeling in the ground truth and assigning higher anomaly scores near the outlier boundaries.

B MORE ANALYSIS ON STAR

B.1 APPLICABILITY FOR DATASET

While most industrial scenarios feature a variety of *state variables*, there are also special or constrained settings where such variables are unavailable. To further extend the applicability of STAR, we explored the approach of proactively constructing pseudo-covariates to serve as *state variables* for processing by the STAR module. Specifically, numerical variables often inherently carry state information. For instance, temperature indicates whether the system is in a high or low-temperature state, while the pH value reflects the precondition of an acidic or alkaline environment. We leverage this property by discretizing these numerical variables into discrete states to construct our pseudo-covariates. We conducted this experiment on the PSM Abdulaal et al. (2021), PUMP Feng & Tian (2021), and ECG Yoon et al. (2020) datasets, and the results are presented in Table 7. Rows marked with an asterisk (*) denote the use of pseudo-covariates. The results indicate that in most cases, the incorporation of *state variables* still leads to a decrease in performance. Although the pseudo-covariates lack a well-defined physical meaning, STAR is nevertheless able to improve the performance of TSFMs to a certain degree.

B.2 VISUALIZATION OF IDENTITY-GUIDED STATE ENCODER

To further validate the effectiveness of the *Identity-guided State Encoder*, we visualized its output embeddings as well as the selections made by the *Memory Router*. We selected the Genesis (von Birgelen & Niggemann, 2018) for our analysis, and a subset of its variables is described in Table B.2. We use Id_v to denote the variable identity (index of *state variable*), and Id_s to denote the state identity (discrete value of *state variable*). Figure 4a illustrates the similarity between embeddings of different variables, where a distinct clustering pattern is observed. This indicates that variables with similar semantic information exhibit higher similarity. Since our router is conditioned on both variable identity and state identity, embeddings for variables that share the same variable identity or state identity exhibit greater similarity. However, the overall influence of variable identity is more pronounced than that of state identity. These observations are further corroborated by Figure 4b.

Table 7: Evaluate STAR on datasets containing solely numerical variables.

Dataset	PSM			PUMP			ECG			
	Metric	A-R	V-R	V-P	A-R	V-R	V-P	A-R	V-R	V-P
DADA		0.606	0.581	0.403	0.775	0.778	0.226	0.839	0.807	0.508
DADA*		0.621	0.588	0.391	0.764	0.777	0.223	0.828	0.801	0.495
+STAR*		0.636	0.592	0.412	0.807	0.807	0.236	0.844	0.811	0.514
UniTS		0.582	0.573	0.377	0.415	0.573	0.211	0.872	0.840	0.522
UniTS*		0.548	0.544	0.354	0.384	0.536	0.195	0.863	0.835	0.516
+STAR*		0.607	0.602	0.401	0.436	0.598	0.217	0.884	0.848	0.537

Table 8: Evaluate STAR on datasets containing solely numerical variables.

Id_v	Group	Variable name	Descriptions
1	Slider State	Slider_OUT	The slider is on the outside.
2		Slider_IN	The slider is on the inside.
3	Detection State	NonMetall	Non-metal detected.
4		Metall	Metal detected.
5	Position State	Pos4reached	Arrived at Position 4.
6		Pos3reached	Arrived at Position 3.
7		Pos2reached	Arrived at Position 2.
8		Pos1reached	Arrived at Position 1.

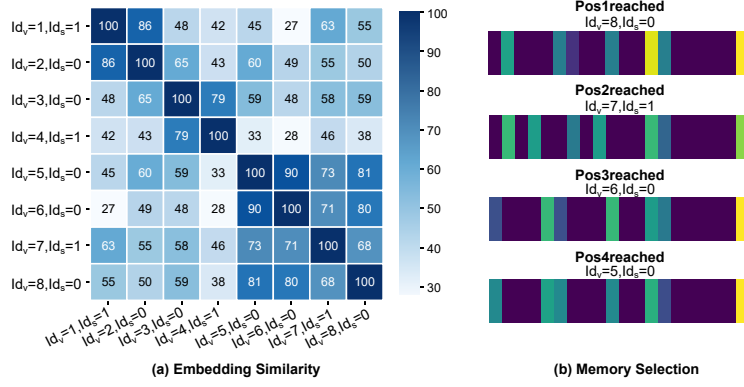


Figure 4: (a) shows the similarity between the embeddings output from *Identity-guided State Encoder*. (b) shows the weight of selection in *Memory Router*.

B.3 CASE STUDY

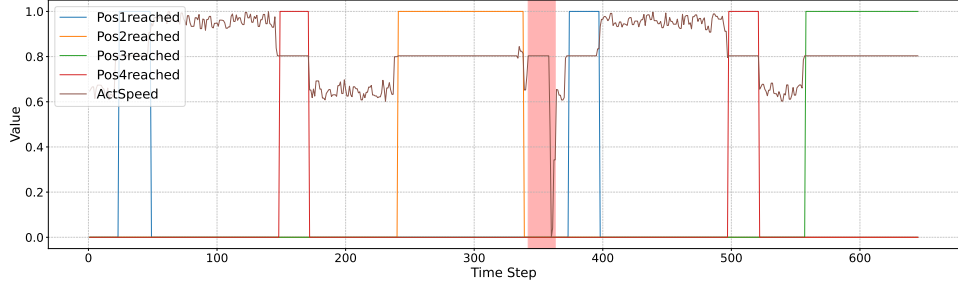


Figure 5: Case series in Genesis.

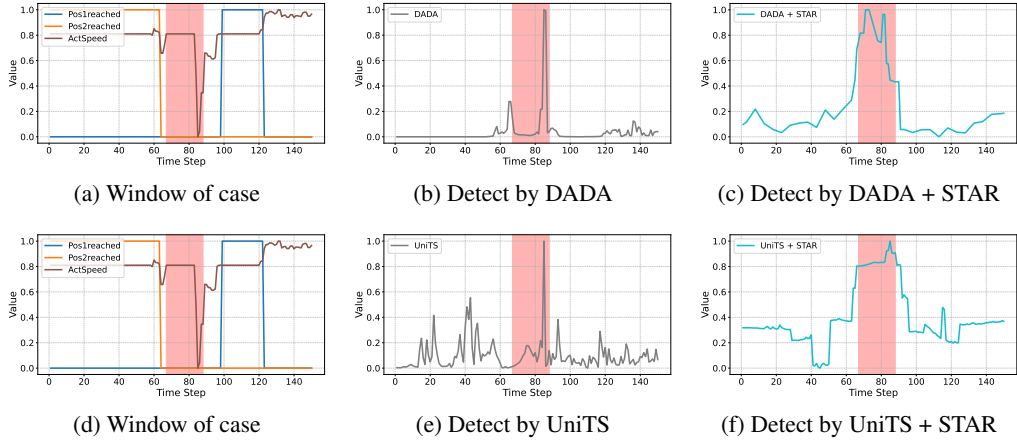


Figure 6: Anomaly score of backbones and STAR in case from Genesis.

To further analyze how STAR works, we selected and visualized cases from real-world datasets.

(1) **Genesis** Figure 5 illustrates that the position state variables (Pos1reached, Pos2reached, and Pos3reached) have a condition-based inference on the actual motor speed (ActSpeed). Under normal circumstances, the actual motor speed exhibits a stable pattern when the system is in a state associated with reaching a specific position (PosXreached = 1). However, when the system is not reached at any specific position, the motor speed displays an unstable pattern (PosXreached = 0).

The anomaly presented in the case is that the actual motor speed exhibits a stable pattern even when the system is in a state of not having reached any specific position. This constitutes a state-value mismatch anomaly. As shown in Figure 6, although TSFMs are highly sensitive to the abrupt

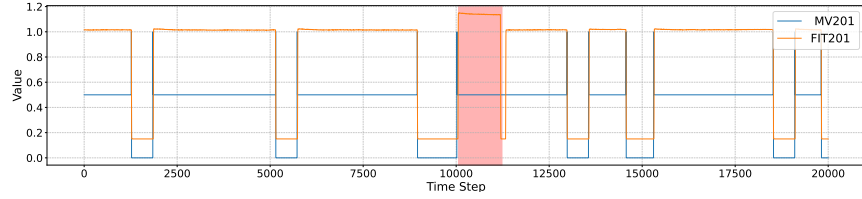


Figure 7: Case series in SWaT.

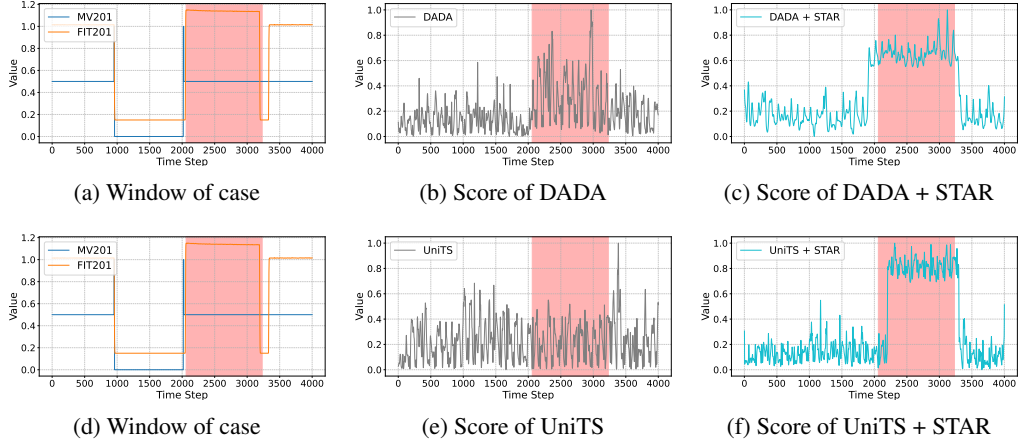


Figure 8: Anomaly score of backbones and STAR in case from SWaT.

change at the final timestamps of the anomaly, they fail to detect the preceding portion. With the integration of STAR, the model gains heightened sensitivity to the state-value mismatch anomaly and successfully captures this anomaly case.

(2) **SWaT** As shown in Figure 5, the state variable of motorized valve switch (MV201) also has a condition-based inference on the water flow (FIT201). Under normal conditions, the behavior is as follows: when the valve is open ($MV201=0.5$), the water flow remains stable at a high level; when the valve is closed ($MV201=0$), the flow stabilizes at a low level; and during a transitional state ($MV201=1$), the flow rapidly increases or decreases.

The anomaly presented in the case is twofold. On the one hand, the water level is excessively high. On the other hand, the flow begins to decrease rapidly even though the valve is not in a transitional state ($MV201=1$), remaining fully open ($MV201=0.5$). Although DADA successfully identified the excessively high water level, it failed to detect the anomaly of the rapid decrease. This is likely because the variable itself frequently exhibits patterns of rapid decline over short periods. STAR successfully captures this anomaly by considering the degree of matching between the state and the numerical value.

C THE USE OF LARGE LANGUAGE MODELS

The use of open-source Large Language Models (LLMs) in this work was strictly limited to assisting with the translation of certain terms and polishing a small portion of the text. LLMs did not contribute to the conceptual aspects of the research, including information retrieval, knowledge discovery, or the ideation process.